Available online at www.sciencedirect.com

ScienceDirect

Journal of Nutritional Biochemistry 46 (2017) 109–116

Journal of Nutritional Biochemistry

Fructose increases corticosterone production in association with NADPH metabolism alterations in rat epididymal white adipose tissue

Paula D. Prince[a,b], Yanina A. Santander[c], Estefania M. Gerez[a], Christian Höcht[c], Ariel H. Polizio[c,d], Marcos A. Mayer[d,e,f], Carlos A. Taira[c,d], Cesar G. Fraga[a,b], Monica Galleano[a,b,1], Andrea Carranza[c,g,*,1]

[a]Universidad de Buenos Aires, Facultad de Farmacia y Bioquímica, Departamento de Química Analítica y Fisicoquímica, Cátedra de Fisicoquímica, Buenos Aires, Argentina
[b]CONICET- Universidad de Buenos Aires, Instituto de Bioquímica y Medicina Molecular (IBIMOL), Buenos Aires, Argentina
[c]Universidad de Buenos Aires, Facultad de Farmacia y Bioquímica, Departamento de Farmacología, Cátedra de Farmacología, Buenos Aires, Argentina
[d]CONICET, Buenos Aires, Argentina
[e]Fundación CESIM, Santa Rosa, La Pampa, Argentina
[f]Universidad de La Pampa, Facultad de Ciencias Naturales, Santa Rosa, La Pampa, Argentina
[g]CONICET-Universidad de Buenos Aires, Instituto de Investigaciones Cardiológicas (ININCA), Buenos Aires, Argentina

Received 21 September 2016; received in revised form 12 January 2017; accepted 25 February 2017

Abstract

Metabolic syndrome is an array of closely metabolic disorders that includes glucose intolerance/insulin resistance, central obesity, dyslipidemia, and hypertension. Fructose, a highly lipogenic sugar, has profound metabolic effects in adipose tissue, and has been associated with the etiopathology of many components of the metabolic syndrome. In adipocytes, the enzyme 11 β-HSD1 amplifies local glucocorticoid production, being a key player in the pathogenesis of central obesity and metabolic syndrome. 11 β-HSD1 reductase activity is dependent on NADPH, a cofactor generated by H6PD inside the endoplasmic reticulum.

Our focus was to explore the effect of fructose overload on epididymal white adipose tissue (EWAT) machinery involved in glucocorticoid production and NADPH and oxidants metabolism.

Male Sprague–Dawley rats fed with a fructose solution (10% (w/v) in tap water) during 9 weeks developed some characteristic features of metabolic syndrome, such as hypertriglyceridemia, and hypertension. In addition, high levels of plasma and EWAT corticosterone were detected. Activities and expressions of H6PD and 11 β-HSD1, NAPDH content, superoxide anion production, expression of NADPH oxidase 2 subunits, and indicators of oxidative metabolism were measured. Fructose overloaded rats showed an increased potential in oxidant production respect to control rats. In parallel, in EWAT from fructose overloaded rats we found higher expression/activity of H6PD and 11 β-HSD1, and NADPH/$NADP^+$ ratio.

Our in vivo results support that fructose overload installs in EWAT conditions favoring glucocorticoid production through higher H6PD expression/activity supplying NADPH for enhanced 11 β-HSD1 expression/activity, becoming this tissue a potential extra-adrenal source of corticosterone under these experimental conditions.

Keywords: Glucocorticoids; Metabolic syndrome; 11 β-Hydroxysteroid dehydrogenase 1; Hexose-6-phosphate dehydrogenase; Fructose

1. Introduction

First characterized by Reaven in the late 1980s [1], the metabolic syndrome (MetS) is described as an array of closely associated metabolic disorders, such as central obesity, hypertension, dyslipidemia, and hyperglycemia/insulin resistance. MetS predisposes to type II diabetes mellitus, atherosclerosis, and cardiovascular complications [2,3]. Intensive research has proposed an important role for hexoses and fatty acids in insulin resistance and β-cell dysfunction [4]. High consumption of dietary fructose, primarily from sucrose and high-fructose corn syrup, has been implicated as a contributing factor to the development of MetS [5,6] through deregulation of many molecular signaling pathways [7].

Glucocorticoids (GCs) are potent regulators of the energy metabolism. The phenotype of the MetS is fairly similar to that of Cushing's syndrome, such as central obesity, glucose intolerance, dyslipidemia and hypertension, suggesting that enhanced GC action may be, at least in part, responsible for the pathogenesis of the syndrome [8]. High intra adipocyte cortisol levels have been proposed to be a major determinant of obesity and MetS in humans, promoting the differentiation of preadipocytes, and decreasing insulin sensitivity [9,10]. Interestingly, rodents under chronic GC exposure develop a phenotype similar to MetS characterized by impaired glucose tolerance, and alterations in the adipose tissue lipid metabolism [11,12].

GC levels are regulated at the pre-receptor level by the enzyme 11 beta-hydroxysteroid dehydrogenase 1 (11 β-HSD1) located in the endoplasmic reticulum (ER) membrane of metabolic tissues such as liver

* Corresponding author at: Universidad de Buenos Aires, Facultad de Farmacia y Bioquímica, Departamento de Farmacología, Cátedra de Farmacología, - Junín 956 5to piso, Buenos Aires, Argentina - C.P.C1113 AAD. Tel.: +54 11 5287 4502.
E-mail address: carranza.ma@gmail.com (A. Carranza).
[1] Share senior supervision.

http://dx.doi.org/10.1016/j.jnutbio.2017.02.021
0955-2863/

and adipose tissue. In vivo, 11 β-HSD1 is a bidirectional and NADPH-dependent enzyme. Predominantly, this enzyme acts as an oxoreductase to regenerate the active GC receptor ligand cortisol (corticosterone in rodents) from the inactive cortisone (11-dehydrocorticosterone in rodents) [13–15]. As the ER membrane is relatively impermeable to pyridine nucleotides, the co-localized enzyme hexose 6 phosphate dehydrogenase (H6PD) plays a critical role in regulating the oxoreductase activity of 11 β-HSD1 by providing the cofactor NADPH within the ER lumen [16,17].

The activity of 11 β-HSD1 is significantly increased in fat tissues from obese humans and rodents [18,19], suggesting that chronically increased 11 β-HSD1 activity induces GC receptor activation and thereby promotes obesity and its associated metabolic complications [20,21].

As was proposed, high nutrient (electron donor) intake of either carbohydrates or lipids can lead to enhanced GC production, especially in insulin-sensitive tissues that counter-regulate insulin action and promotes nutrient storage, hence producing the most characteristic features of the MetS [13,20]. In parallel, this high nutrient intake would modify the oxidant/antioxidant balance considering that supplies reducing equivalents for oxidant-producing systems, as NADPH oxidases (NOX), and antioxidant systems, as glutathione (GSH) and GSH-dependent detoxifying enzymes [22]. The final scenario of these modifications in oxidative metabolism is organ-specific and for adipose tissue is still not completely understood [23,24].

Fructose overload has been proposed as a pathogenic cause of MetS. However, it is not completely understood how fructose predisposes to it. In line with this, the present study was designed to evaluate if MetS developed in rats by fructose overload could be related to an overproduction of GC and to explore the mechanisms involved in terms of corticosterone, NADPH and oxidants metabolism.

2. Materials and methods

2.1. Animals and treatment

All procedures were in agreement with the "International Guiding Principles for Biomedical Research Involving Animals 2012" performed by the International Council for Laboratory Animal Science (CIOMS-ICLAS) and were approved by the local Institutional Committee for the Care and Use of Experimental Animals, School of Pharmacy and Biochemistry, University of Buenos Aires (Exp UBA 15097/2015).

Two months old Sprague Dawley rats weighing 150±20 g were housed under conditions of controlled temperature (21–25°C) and humidity, with a 12 h light/dark cycle. After one week of acclimatization, rats were divided into two groups (eight rats per group): control group (C-fed) received tap water ad libitum and standard rat chow diet in pellets with the following composition (w/w): 20% protein, 3% fat, 2% fiber, 6% minerals and 69% starch and vitamins supplying 13.8 KJ/g (Asociación Cooperativas Argentinas, Campana, Buenos Aires, Argentina) and fructose group (F-fed) received fructose 10% (w/v) in the drinking water and standard rat chow diet during 9 weeks. At the end of the treatment, food and liquid intakes were measured and caloric intake for C-fed rats was calculated as energy ingested as food [food weight (g) × 13.8 KJ/g], while caloric intake for F-fed rats was calculated as the addition of energy ingested as food and fructose solution [food weight (g) × 13.8 KJ/g + fructose intake (ml) × 1.67 KJ/ml].

2.2. Blood pressure determination

Rats were trained to the procedure of indirect systolic blood pressure measurement by the tail cuff method during 2 weeks prior to the sacrifice. The day before the sacrifice, systolic blood pressure was measured using a microphone connected to a Grass D.C. driver amplifier (model 7DAC, Grass Instruments, Quincy, MA, USA) in series with a Grass polygraph (model 79D, Grass Instruments, Quincy, MA, USA). The mean of three to four consecutive readings was used as the reported value of systolic blood pressure for each rat.

2.3. Plasma and tissue collection

At the end of the treatment and after overnight fast, the rats were weighed, anesthetized with ketamine (50 mg/kg) and xylazine (1 mg/kg), and blood was collected by cardiac puncture with a heparinized syringe before euthanasia by decapitation. Plasma obtained by blood centrifugation (3,500xg at 4°C for 10 min) was frozen at −80°C for further analysis. Plasma glucose and triglyceride (TG) levels were measured by means of spectrophotometry (Metrolab 325 bd, spectrophotometer UV-Vis, Argentina) with commercial kits for glycaemia (GOD/POD, enzymatic method) and triglyceridemia (Color GPO/PAP AA), from Wiener Labs (Rosario, Santa Fe, Argentina). Epididymal white adipose tissue (EWAT) was excised, weighed and immediately frozen at −80°C for later determinations of enzymatic activities, TG content and Western blot analysis.

Table 1
General parameters and systolic blood pressure.

Parameter	C-fed	F-fed
Food intake (g/day)	23±3	16±4*
Liquid intake (ml/day)	14±2	50±5*
Caloric intake (KJ/day)	318±29	304±54
Body weight (g)	370±10	377±11
EWAT weight (g)	2.6±0.2	3.5±0.2*
EWAT weight/body weight ($x10^3$)	7.0±0.7	9.2±0.1*
Systolic blood pressure (mmHg)	114±1	129±1*

Rat general parameters were measured after 9 weeks of treatment in C-fed rats (chow and tap water) and F-fed rats (chow and 10% fructose (w/v) in the drinking water). Data are presented as mean±S.E.M. (n=8 per group).
*p<0.05 F-fed vs. C-fed rats was considered statistically significant. EWAT, epididymal white adipose tissue.

2.4. EWAT TG content

EWAT was homogenized in 5 % (v/v) of Triton-X100 in distilled water (0.1 g/ml) and boiled three times before centrifugation at 10,000xg for 2 min. The supernatant was diluted 1:5 in the homogenization buffer and TG levels were measured [25].

2.5. Adipose tissue corticosterone detection

EWAT was homogenized in 1 vol (w/v) of PBS buffer (7.6 mM KH_2PO_4, 42.4 mM K_2HPO_4, 150 mM NaCl, pH 7.4) using a manual homogenizer (PRO Scientific Inc., CT, USA) and centrifuged at 600×g for 15 min at 4°C. 400 μl of the homogenate containing internal standard (5 nM cortisone) were shaken for 30 s with 2 ml of ethyl acetate and centrifuged at 2,000×g for 10 min at 4°C. The organic phase was transferred to a glass tube and 1 ml of hexane and 1 ml of methanol:H_2O (7:2) were added, shaken for 30 s and centrifuged at 2,000×g for 10 min at 4°C. The hexane phase was aspirated to waste and the aqueous methanol phase was evaporated under nitrogen at 40°C to dryness [26]. The residue was dissolved in 200 μl of mobile phase [acetonitrile:H_2O (30:70)] and separated by HPLC-UV (Waters 515 HPLC Pump coupled to an UV detector 250 nm, UVIS 204 from Linear Instruments, Reno, NV, USA) using a Phenomenex Luna 5 μm, C18, 150 mm × 4.60 mm column (Phenomenex, Torrance, CA, USA). Analytes identification was done by using corticosterone standards (Sigma Aldrich Chemical Co., St. Louis, MO, USA). The quantification limit of endogenous corticosterone was 20 ng/ml and the method was linear in the range of 20–500 ng/ml [27].

2.6. Plasma corticosterone determination

Plasma concentrations of corticosterone were quantified by means of HPLC-UV detection. Plasma corticosterone was extracted from 1 ml of sample with 100 μl of internal standard (cortisone 1 μg/ml) and 4 ml ethyl ether:dichloromethane (60:40). The mixture was shaken for 30 s and centrifuged at 2,000×g for 5 min. The organic layer was transferred into a conical tube and evaporated under nitrogen gas. The dry extract was reconstituted with mobile phase [acetonitrile:H_2O (30:70)] and separated by HPLC-UV as depicted above.

2.7. Indicators of oxidative metabolism

Butylhydroxytoluene (BHT, 1% (w/v) final concentration) was added to plasma aliquots to fluorometrically determine thiobarbituric acid reactive species (TBARS) content using butanol to extract the complex formed according to Fraga et al. (1987) [28]. 1,1,3,3-Tetramethoxypropane was used to prepare the standard of malondialdehyde (MDA). The results were expressed as content of MDA (μM). Plasma α-tocopherol (α-TP) was extracted with hexane and quantified by reverse phase HPLC-ED (Coloumchem II, ESA Inc., Bedford, MA, USA) at an applied oxidation potential of +0.6 V [29]. The oxidation of

Table 2
Metabolic parameters.

Parameter	C-fed	F-fed
Fasting plasma glucose (mmol/l)	5.6±0.2	6.1±0.7
Plasma TG (mmol/l)	1.0±0.2	1.8±0.2*
Plasma corticosterone (nmol/l)	260±40	549±60*
EWAT TG (μmol/g)	92 ±12	173±22*

Parameters were measured after 9 weeks of treatment in C-fed rats (chow and tap water) and F-fed rats (chow and 10% fructose (w/v) in the drinking water). Data are presented as means±S.E.M. (n=8 per group).
*p<0.05 F-fed vs. C-fed rats was considered statistically significant. TG, triglycerides; EWAT, epididymal white adipose tissue.

Table 3
Oxidative metabolism.

Parameter	C-fed	F-fed
Plasma		
TBARS (μmol MDA/l)	1.31±0.05	1.37±0.03
Carbonyl groups (nmol/mg protein)	6.1±0.6	6.0±0.3
α-TP/TG (nmol/mmol TG)	23±3	12±2*
EWAT		
TBARS (nmol MDA/mg protein)	0.6±0.2	0.6±0.1
GSH content (μmol/mg protein)	68±7	37.1±1.0*
SOD activity (Units/mg protein)	7±2	7±1
CAT activity (nmol/mg protein.min)	15±5	15±3
GR activity (nmol/mg protein.min)	20±2	18±1
GPx activity (nmol NADPH ox/mg protein.min)	87±10	52±5*

Oxidative metabolism-related parameters were measured after 9 weeks of treatment in C-fed rats (chow and tap water) and F-fed rats (chow and 10% fructose (w/v) in the drinking water). Data are presented as means±S.E.M. (n=8 per group).
*p<0.05 F-fed vs. C-fed rats was considered statistically significant. TBARS, thiobarbituric acid reactive species; MDA, malondialdehyde; α-TP, α-tocopherol; TG, triglycerides; GSH, reduced glutathione; SOD, superoxide dismutase; CAT, catalase; GR, glutathione reductase; GPx, glutathione peroxidase.

plasma proteins was determined spectrophotometrically through the reaction with 2,4-dinitrophenylhydrazine, to detect carbonyl groups [30].

EWAT was homogenized in 154 mM KCl, pH 7.4 containing 3 mM EDTA and sonicated for 30 s at 4°C. Samples were centrifuged at 600×g for 10 min at 4°C and supernatants were delipidated and used to measure TBARS, total glutathione content, and enzymatic activities. TBARS content was measured as detailed above and expressed as MDA content (nmol/mg prot). Total glutathione content [reduced (GSH) and oxidized (GSSG)] was determined spectrophotometrically after precipitation with 2% (v/v) perchloric acid. The reaction was carried out using yeast-glutathione reductase (GR), 5,5′ dithio-bis-(2-nitrobenzoic acid) and NADPH, reading the absorbance at 340 nm. GSSG was determined in the presence of 2-vinylpyridine, and GSH was calculated from the difference between total glutathione and GSSG [31]. Superoxide dismutase (SOD) activity was spectrophotometrically determined, following the inhibition of adrenochrome [32]. Catalase (CAT) activity was determined spectrophotometrically following the consumption of H_2O_2 at 240 nm [33]. GR activity was measured according to Carlberg and Mannervik (1985) [34], with modifications: samples were incubated in 10 mM Tris–HCl buffer pH 7.0 in the presence of 0.5 mM GSSG and 0.15 mM NADPH and the oxidation of NADPH was followed spectrophotometrically at 340 nm. Glutathione peroxidase (GPx) activity was determined spectrophotometrically following the enzymatic oxidation of NADPH at 340 nm in the presence of 1 mM GSH, 1 mM NaN_3, 0.15 mM NADPH and 0.25 U/ml GR [35].

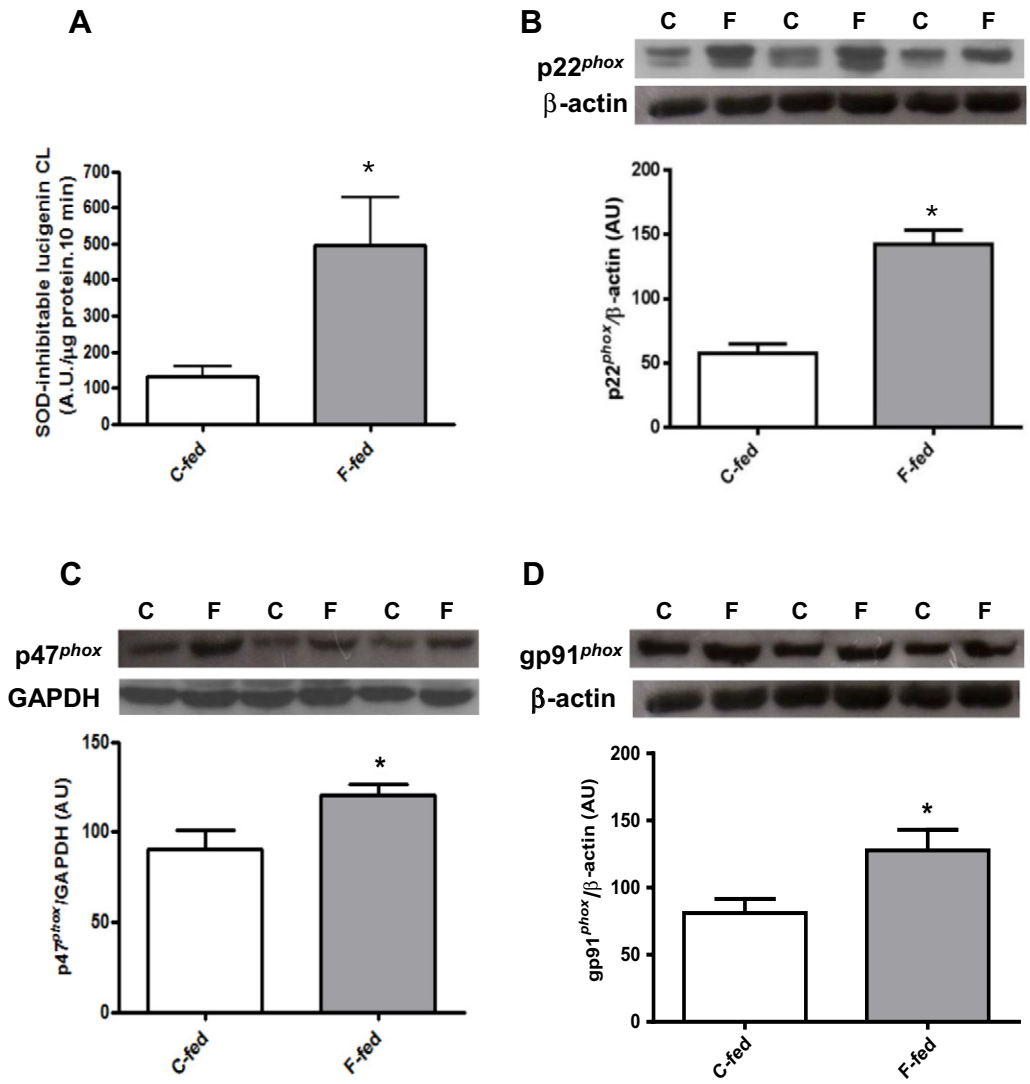

Fig. 1. Fructose diet increases NADPH-dependent superoxide anion production and the expressions of NOX2 subunits $p22^{phox}$, $p47^{phox}$ and $gp91^{phox}$ in EWAT. (A) Superoxide anion production was measured as the SOD-inhibitable chemiluminescence (CL) of lucigenin in the presence of NADPH in mitochondria-free homogenates of EWAT. Expression of NOX2 subunits (B) $p22^{phox}$, (C) $p47^{phox}$ and (D) $gp91^{phox}$ were analyzed by Western blot in EWAT homogenates. Representative immunoblots of three experiments in triplicate and graphical representations of protein expressions normalized to the amount of β-actin or GAPDH estimated by densitometric analysis are shown. Data are presented as means±S.E.M. (n=8 animals per group). *p<0.05 F-fed vs. C-fed rats was considered statistically significant.

2.8. Determination of NADPH-dependent superoxide anion production

EWAT was homogenized in PBS buffer (7.6 mM KH_2PO_4, 42.4 mM K_2HPO_4, 150 mM NaCl, pH 7.4) and centrifuged at 600×*g* for 20 min at 4°C. Supernatants were delipidated and centrifuged at 10,000×*g* for 20 min at 4°C to obtain mitochondria-free homogenates, used to measure lucigenin-enhanced chemiluminescence [36]. Briefly, samples were added to vials containing 1 ml of warm (37°C) 50 mM potassium phosphate buffer pH 7.4 containing 5 μM lucigenin and 40 μM NADPH in the absence and the presence of 200 U/ml SOD. Light emission was measured each 10 s for 10 min using a LKB Wallac 1209 Rackbeta Liquid Scintillation Counter (Turku, Finland) in the chemiluminescence mode, and the area under the curve was calculated. The results were expressed as arbitrary units (A.U./μg protein.10 min).

2.9. Analysis of NADPH oxidase 2 (NOX2) subunits expressions

EWAT was homogenized in 1 vol (w/v) of ice-cold homogenization buffer (150 mM NaCl, 50 mM, Trizma–HCl pH 8.0 containing 1% (v/v) sodium deoxycholate, 1 mM EGTA, 1 mM NaF, 1 mM phenylmethanesulfonylfluoride and 1 mM sodium pervanadate), and a protease inhibitor cocktail 4% (Roche, Hertfordshire, UK). Samples were centrifuged at 10,000×*g* for 20 min at 4°C to discard cellular debris and nucleus. Supernatants were delipidated and resuspended in 2X solution of SDS-sample buffer (62.5 mM Tris–HCl buffer pH 6.8 containing 2% (w/v) SDS, 25% (w/v) glycerol, 5% (v/v) β-mercaptoethanol and 0.01% (w/v) bromophenol blue) and heated at 95°C for 5 min. Protein extracts were quantified by the Lowry method and equal amount of proteins (60 μg) was loaded onto 10% SDS-PAGE and transferred to PVDF membranes. After blocking for 1 h in 5% (w/v) nonfat milk, membranes were incubated overnight at 4°C with the corresponding primary antibodies (gp91^{phox} (#5827), p47^{phox} (#7660), p22^{phox} (#11712), GAPDH (#25778), and β-actin (#47778) from Santa Cruz Biotech Inc., Dallas, TX, USA) (1:1,000 in PBS buffer). After incubation for 90 min at room temperature with the corresponding HRP-conjugated secondary antibodies (rabbit anti-goat IgG-HRP (#2768), mouse anti-rabbit IgG-HRP (#2357), and goat anti-mouse IgG-HRP (#2005) from Santa Cruz Biotech Inc., Dallas, TX, USA) (1:5,000 in PBS buffer), complexes were visualized by chemiluminescence detection (Pierce ECL Western blotting Substrate). Densitometry analysis of the bands was performed using Image J (National Institute of Health, Bethesda, MD, USA). Protein band densities were normalized to the β-actin or GAPDH content.

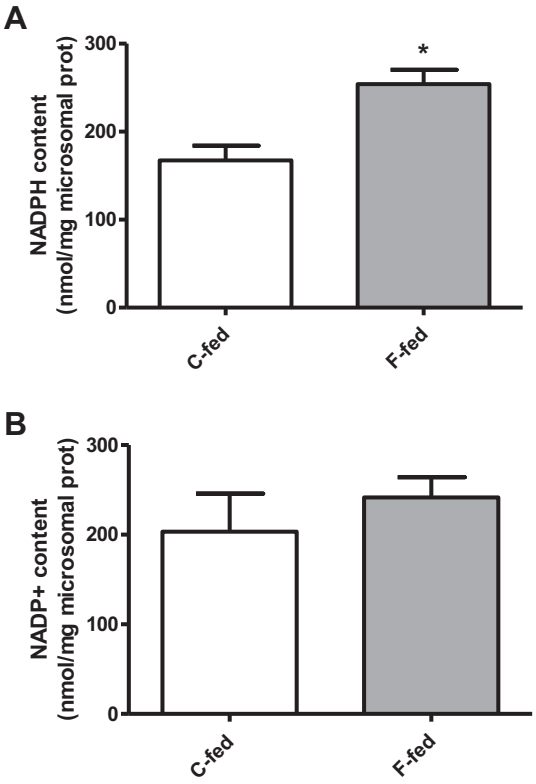

Fig. 2. Fructose diet increases microsomal NADPH content in EWAT. Endogenous (A) NADPH and (B) NADP$^+$ contents were measured spectrophotometrically in microsomal fractions of EWAT. Results are expressed as mean±S.E.M. (n=8 per group). *p<0.05 F-fed vs. C-fed rats was considered statistically significant.

2.10. Determination of cytosolic G6PD activity and microsomal NADPH and NADP$^+$ contents

For the subcellular fractions isolation, 0.5 g of frozen EWAT was homogenized in 1 ml of homogenization buffer (30 mM Tris–HCl pH 7.4 containing 0.9 mM EDTA, 300 mM sucrose, and 1 mM GSH) [37]. The homogenates were centrifuged at 16,000×*g* for 15 min at 4°C. Pellets were discarded and the supernatants were delipidated and centrifuged at 65,000×*g* for 1 h at 4°C to obtain the cytosolic and the microsomal fractions [38].

Glucose 6 phosphate dehydrogenase (G6PD) activity was measured spectrophotometrically in the cytosolic fraction by detection of NADPH formation at 340 nm from aliquots with 50 μg of protein in reaction buffer [100 mM glycylglycine pH 7.6 containing 10 mM $MgCl_2$, 0.2 mM NADP$^+$ and 2 mM glucose 6 phosphate (G6P)] [37]. NADPH and NADP$^+$ contents were determined in the microsomal fractions as described previously [39,40].

2.11. Determination of H6PD and 11 β-HSD1 activities and expressions

The enzymatic activities were measured in the microsomal fraction according to Tian et al. by measuring the increase in the absorbance at 340 nm due to the conversion of NADP$^+$ to NADPH in a Beckman Coulter TM DU 7400 spectrophotometer (Canton, MA, USA). Considering that in the pentose phosphate pathway both H6PD and 6 phosphogluconate dehydrogenase (6PGD) produce NADPH, the 6PGD activity alone and the total dehydrogenase activity (H6PD plus 6PGD) were measured separately. Thus, the activity of H6PD was calculated by subtracting the activity of 6PGD to the total dehydrogenase activity [39]. To assay the enzymatic activities, 20 μl of microsomes (1 μg/μl) were added to a cuvette containing 50 mM Tris buffer pH 8.1, 1 mM $MgCl_2$ and 0.1 mM NADP$^+$ in the presence of 0.2 mM glucose 6-phosphate and 0.2 mM 6-phosphogluconate to obtain total dehydrogenase activity, or in the presence of 0.2 mM 6-phosphogluconate to assess the activity of 6PGD [41].

11 β-HSD1 activity was measured spectrophotometrically according to Tian et al. following NADPH consumption at 340 nm [41]. Briefly, 20 μl of microsomes (1 μg/μl)

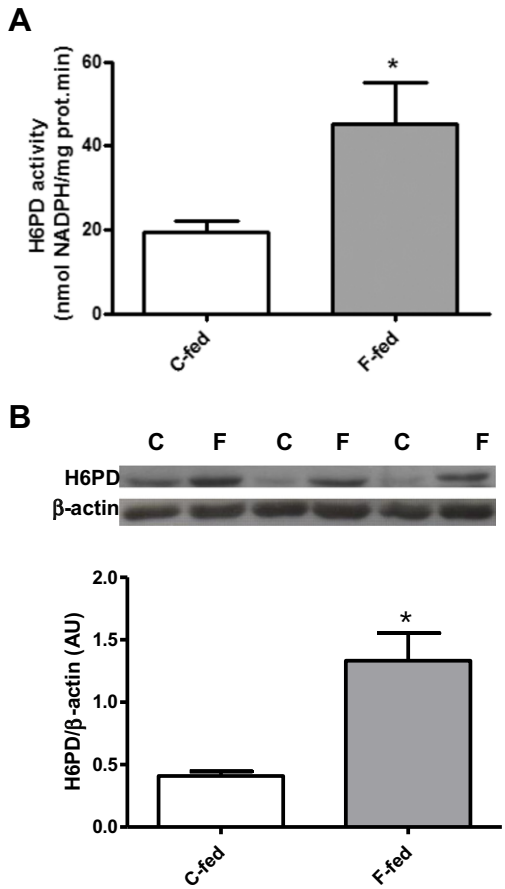

Fig. 3. H6PD activity and expression are increased in EWAT of F-fed rats. (A) H6PD activity was measured spectrophotometrically in microsomal fractions of EWAT. (B) Expression of H6PD was measured by Western blot in EWAT microsomal fractions. Representative immunoblots of three experiments in triplicate and graphical representations of protein expressions normalized to the amount of β-actin estimated by densitometric analysis are shown. Data are presented as means±S.E.M. (n=8 animals per group). *p<0.05 F-fed vs. C-fed rats was considered statistically significant.

were added to a cuvette containing 50 mM Tris buffer pH 8.1, 1 mM $MgCl_2$, 2 mM NADPH in the presence of 100 μM cortisone because cortisone is also a good substrate for the rat 11 β-HSD1 enzyme [15].

For the determination of H6PD and 11 β-HSD1 expressions in microsomes, EWAT was homogenized as indicated in 2.10 and the microsomal fraction was isolated and processed for Western blot analysis as described previously in 2.9. The primary antibodies were 11 β-HSD1 (#20175), H6PD (#67394), and β-actin (#47778) from Santa Cruz Biotech Inc., Dallas, TX, USA (1:1,000 in PBS buffer).

2.12. Statistical analysis

All data are expressed as means±S.E.M. Differences between groups were analyzed by Student's *t* test using Graph Pad Prism 6 software. Differences were considered statistically significant at $p<0.05$ or less (C-fed vs. F-fed).

3. Results

3.1. Food intake, body weight and metabolic parameters in C-fed and F-fed animals

At the end of the treatment, total body mass was similar between C-fed rats and F-fed rats. However, EWAT weight and its relative ratio to total body weight were significantly higher in F-fed rats, suggesting that fructose overload induces adipogenesis and/or adipocyte hypertrophy. In F-fed rats compared to C-fed rats, the food intake was significantly lower meanwhile the fluid intake was significantly higher. The total energy intake was unchanged between groups, suggesting a balance between fructose consumption and solid diet intake. In addition, systolic blood pressure was significantly higher in F-fed rats compared to C-fed rats (Table 1).

Table 2 shows the metabolic parameters studied in plasma after 9 weeks of treatment. Plasma fasting glucose remained unchanged, while TG showed a significant increase in plasma from F-fed rats compared to C-fed rats. Interestingly, fructose overload led to significantly higher levels of plasma corticosterone. EWAT TG levels in F-fed group were significantly higher respect to C-fed rats, suggesting that fructose diet increases energy accumulation in EWAT (Table 2).

3.2. Oxidative metabolism

We found no significant differences either in TBARS or in carbonyl levels measured in plasma between the groups. Plasma ratio α-TP/TG levels were significantly lower in F-fed rats compared to control rats suggesting that plasma from F-fed rats were less protected against lipid peroxidation.

In terms of markers of oxidative damage, although TBARS in EWAT showed no differences, total GSH content was significantly lower in F-fed rats compared to C-fed rats. Activities of the antioxidant enzymes SOD, CAT and GR measured in EWAT were not affected by the treatment; meanwhile GPx activity was significantly lower. These results suggest a decreased capacity of EWAT to eliminate a potential excess in hydrogen/organic peroxides production (Table 3).

NADPH-dependent superoxide anion production and the expressions of NOX2 subunits $p22^{phox}$, $p47^{phox}$ and $gp91^{phox}$ were significantly higher in EWAT of F-fed rats compared to C-fed rats. These results indicate a potential up-regulation of NOX2 activity by fructose overload in EWAT (Fig. 1). G6PD activity, the most important regulator of the cytosolic NADPH level, was significantly higher in F-fed rats respect to the control group (C-fed: 3.0±0.2; F-fed: 4.7±0.5 nmol NADPH/mg prot.min, $p<0.05$), suggesting a higher supply of this substrate for all the enzymes requiring NADPH as electron donor in vivo.

3.3. Corticosterone metabolism in adipose tissue

In adipocytes, it was proposed that a hexokinase catalyzes the phosphorylation of fructose to fructose 6 phosphate (F6P) [42], which is transported into the microsomes, where it is isomerized to G6P for H6PD activity [43]. We measured H6PD activity/expression and NADPH content in microsomes isolated from EWAT of both experimental groups. Respect to C-fed animals, NADPH microsomal content was higher in F-fed rats, suggesting a higher H6PD activity within the ER of adipose tissue in F-fed rats (Fig. 2). In line with this, the activity and expression of H6PD were significantly higher in microsomes from F-fed rats respect to C-fed animals (Fig. 3).

It has been demonstrated that active GCs are generated by the oxoreductase activity of the 11 β-HSD1 in the ER from adipocytes incubated with F6P [43]. We measured the activity and expression of 11 β-HSD1 in EWAT microsomes obtained from both experimental groups.

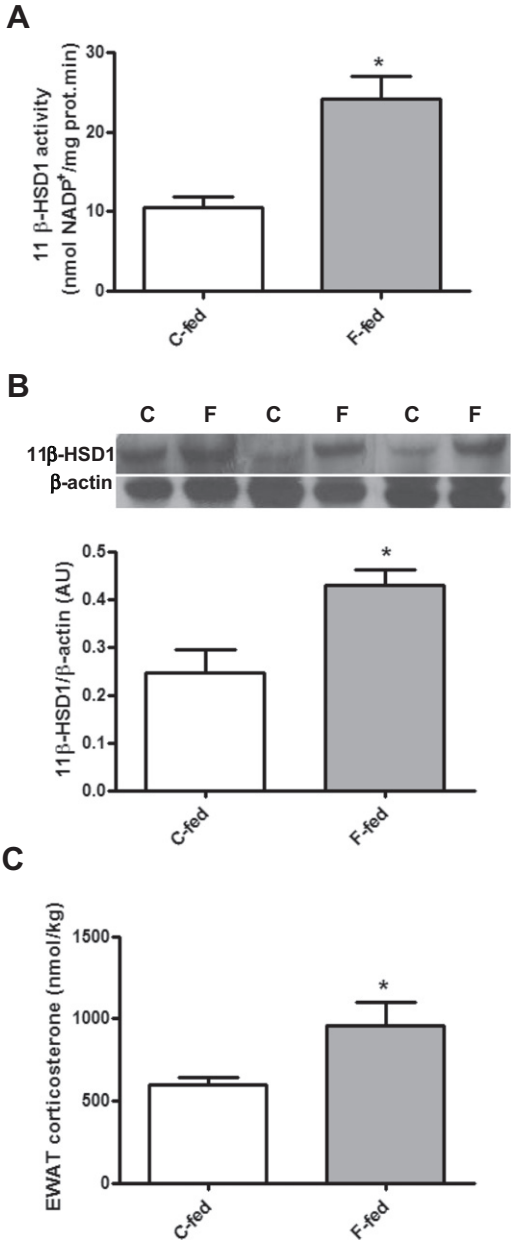

Fig. 4. 11 β-HSD1 oxo-reductase activity and expression, and corticosterone levels are increased in EWAT of F-fed rats. (A) 11 β-HSD1 activity was measured spectrophotometrically in microsomal fractions of EWAT. (B) Expression of 11 β-HSD1 was measured by Western blot in EWAT microsomal fractions. Representative immunoblots of three experiments in triplicate and graphical representations of protein expressions normalized to the amount of β-actin estimated by densitometric analysis are shown. (C) Corticosterone levels were measured in EWAT by HPLC-UV. Results are expressed as mean±S.E.M. ($n=8$ per group). *$p<0.05$ F-fed vs. C-fed rats was considered statistically significant.

The results showed higher activity and expression of 11 β-HSD1 in F-fed rats respect to C-fed group. In accordance, EWAT corticosterone content was significantly increased in EWAT from F-fed animals respect to C-fed animals (Fig. 4).

4. Discussion

Our focus was to explore the effect of fructose overload on EWAT machinery involved in GC production. We observed higher concentrations of corticosterone in EWAT from animals under fructose overload, concomitantly with an increase of microsomal H6PD and 11 β-HSD1 activities and expressions, subtending the hypothesis that fructose overload increases GC production in EWAT.

In this experimental model, the increased fructose consumption was accompanied by a compensatory decrease in chow intake, inducing no change in total energy intake. Although fructose overload did not induce obesity, we reported an increased EWAT mass and TG accumulation, which is consistent with hypertrophic adipose tissue induced by fructose overload reported elsewhere [44]. A key aspect of fructose metabolism is that its entry into the cell via fructokinase bypasses the main rate-controlling step of glycolysis catalyzed by phosphofructokinase, favoring esterification of fatty acids, facilitating VLDL and TG production [45]. Thus, fructose affects the balance between lipolysis and lipogenesis, and this appears to be a major factor to induce hypertriglyceridemia in the postprandial state [46,47]. Increased systolic blood pressure is usually reported in fructose fed animals, and the excess in corticoid production has been postulated as one of the factors involved in blood pressure disturbances [48].

Complex modifications in oxidative metabolism are intimately associated with adipogenesis. Increases in superoxide anion and hydrogen peroxide production are present in terminal adipocyte differentiation and specific roles have been proposed for mitochondria and NOX4 [49,50]. Increased lipogenesis is associated with a controlled oxidants production, for example by NOX2, present in preadipocytes and differentiated adipocytes [24]. In line with this, under our experimental conditions, the indicators of the oxidative metabolism were only partially affected. Interestingly, G6PD activity, a cytosolic NADPH supplier, that was higher in fructose fed animals, was suggested as a promoter of pro-oxidative pathways in the adipose tissue of obese subjects [51]. These data, together with the increased

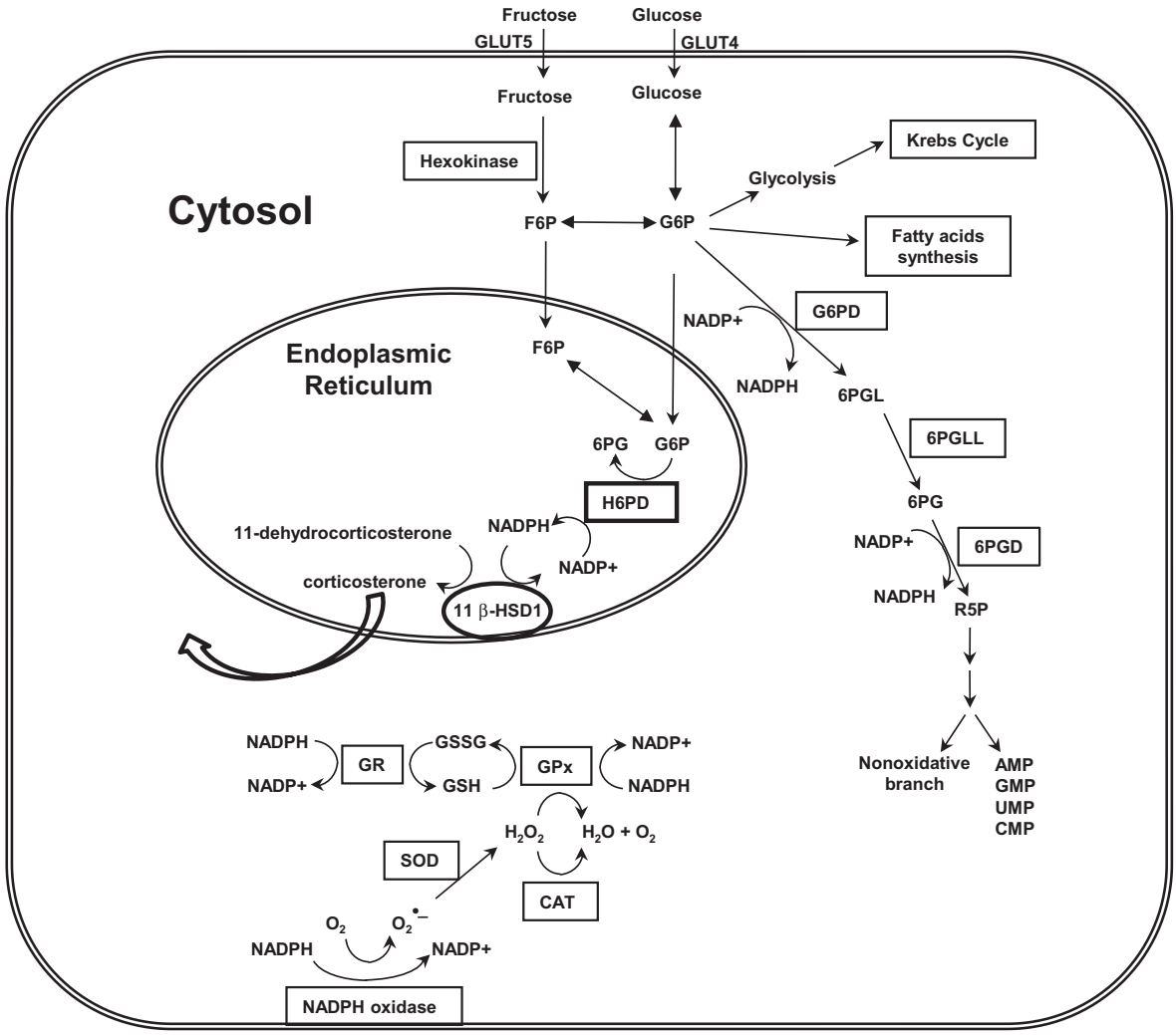

Fig. 5. Schematic representation of corticosterone, NADPH and oxidants metabolism aspects potentially affected by fructose overload in adipocytes. In the adipocyte, fructose is phosphorylated by a hexokinase to F6P, bypasses the main control step (phosphofructokinase) to enter both the glycolysis and the pentose phosphate pathways. Thus, fructose serves as an unregulated source for free fatty acid and monophosphate nucleotides production. The NADPH generated during the pentose phosphate pathway produces reducing equivalents for oxidant production derived from NADPH-dependent oxidases and for GSH-dependent detoxifying enzymes. In the ER lumen, a hexose-phosphate isomerase converts F6P into G6P, substrate of the H6PD that generates NADPH necessary for the oxo-reductase activity of the 11 β-HSD1, favoring corticosterone production.

ex vivo superoxide anion production and NOX2 subunits expressions in EWAT from fructose fed rats suggest a potential in vivo capacity for a substantially increased oxidants production under the adequate substrates/cofactors supply. However, in addition to the lack of manifestation of systemic oxidative stress, EWAT did not show increased lipid peroxidation, probably at the expense of GSH consumption, suggesting a situation of controlled oxidants production compatible with increased lipogenesis.

As fructokinase is not expressed in adipocyte cytosol, fructose is metabolized by a hexokinase to F6P, which is transported to the ER lumen. There, a luminal hexose-phosphate isomerase converts F6P into G6P, substrate of the H6PD that generates NADPH necessary for the 11 β-HSD1 oxoreductase activity [43]. The switch from dehydrogenase to oxoreductase activity of 11 β-HSD1 is associated to the microsomal redox potential due to changes in the NADPH/$NADP^+$ ratio [52]. It has been proposed that the up-regulation of H6PD to generate NADPH stimulates the local production of GC by 11 β-HSD1 [53] (Fig. 5).

Since 11 β-HSD1 is co-located with GC receptors in many cells, it is ideally positioned to amplify the local GC effects [21]. Increased 11 β-HSD1 activity/expression in the adipose tissue may be one of the key events in the development of the MetS subtending the pathogenic role of GC in insulin resistance [20]. Recently, fructose was found to be superior to glucose in promoting the differentiation of 3T3-adipocytes and in enhancing 11 β-HSD1 activity [54]. Moreover, transgenic mice overexpressing 11 β-HSD1 selectively in adipose tissue had increased adipose levels of corticosterone and visceral obesity, insulin resistant diabetes, hyperlipidemia and hyperphagia [9]. As was previously reported, fructose consumption increased 11 β-HSD1 and H6PD expressions and elevated corticosterone level within the adipose tissue [55–57].

In summary, we showed that fructose overload led to the expansion of EWAT, concomitantly with the development of a controlled increment in oxidant production and with alterations in NADPH metabolism associated with increased GC production. In the context of the hypothesis established by Senesi et al. (2010) [43] using in vitro experiments, our results support that fructose overload in vivo installs in EWAT conditions favoring GC production through higher H6PD expression/activity, supplying NADPH for enhanced 11 β-HSD1 expression/activity. Under these experimental conditions, fructose could be a potential reducing equivalent donor for conversion to corticosterone in EWAT pointing it as one of the possible factors in the pathogenesis of the MetS.

Disclosure statement

No conflict of interest.

Funding

This work was supported by CONICET (PIP 11220110101158 to Maria Andrea Carranza and PIP 11220110100612 to Cesar Guillermo Fraga), ANPCyT (PICT 2012-0765 to Cesar Guillermo Fraga), and grants from the University of Buenos Aires (UBACyT 20020100100659 to Monica Galleano and UBACyT 20020120100177 to Cesar Guillermo Fraga), Argentina.

References

[1] Reaven GM. Banting lecture 1988. Role of insulin resistance in human disease. Diabetes 1988;37:1595–607.
[2] Eckel RH, Grundy SM, Zimmet PZ. The metabolic syndrome. Lancet 2005;365:1415–28. http://dx.doi.org/10.1016/S0140-6736(05)66378-7.
[3] Saltiel AR, Kahn CR. Insulin signalling and the regulation of glucose and lipid metabolism. Nature 2001;414:799–806. http://dx.doi.org/10.1038/414799a.
[4] Kahn SE, Cooper ME, Del Prato S. Pathophysiology and treatment of type 2 diabetes: perspectives on the past, present, and future. Lancet 2014;383:1068–83. http://dx.doi.org/10.1016/S0140-6736(13)62154-6.
[5] Bray GA. Energy and fructose from beverages sweetened with sugar or high-fructose corn syrup pose a health risk for some people. Adv Nutr 2013;4:220–5. http://dx.doi.org/10.3945/an.112.002816.
[6] Dekker MJ, Su Q, Baker C, Rutledge AC, Adeli K. Fructose: a highly lipogenic nutrient implicated in insulin resistance, hepatic steatosis, and the metabolic syndrome. Am J Physiol Endocrinol Metab 2010;299:E685–94. http://dx.doi.org/10.1152/ajpendo.00283.2010.
[7] Rutledge AC, Adeli K. Fructose and the metabolic syndrome: pathophysiology and molecular mechanisms. Nutr Rev 2007;65:S13–23.
[8] Bujalska IJ, Kumar S, Stewart PM. Does central obesity reflect "Cushing's disease of the omentum"? Lancet 1997;349:1210–3. http://dx.doi.org/10.1016/S0140-6736(96)11222-8.
[9] Masuzaki H, Paterson J, Shinyama H, Morton NM, Mullins JJ, Seckl JR, et al. A transgenic model of visceral obesity and the metabolic syndrome. Science 2001;294:2166–70. http://dx.doi.org/10.1126/science.1066285.
[10] Tomlinson JW, Finney J, Gay C, Hughes BA, Hughes SV, Stewart PM. Impaired glucose tolerance and insulin resistance are associated with increased adipose 11beta-hydroxysteroid dehydrogenase type 1 expression and elevated hepatic 5alpha-reductase activity. Diabetes 2008;57:2652–60. http://dx.doi.org/10.2337/db08-0495.
[11] Campbell JE, Peckett AJ, D'souza AM, Hawke TJ, Riddell MC. Adipogenic and lipolytic effects of chronic glucocorticoid exposure. Am J Physiol Cell Physiol 2011;300:C198–209. http://dx.doi.org/10.1152/ajpcell.00045.2010.
[12] Karatsoreos IN, Bhagat SM, Bowles NP, Weil ZM, Pfaff DW, McEwen BS. Endocrine and physiological changes in response to chronic corticosterone: a potential model of the metabolic syndrome in mouse. Endocrinology 2010;151:2117–27. http://dx.doi.org/10.1210/en.2009-1436.
[13] Bánhegyi G, Csala M, Benedetti A. Hexose-6-phosphate dehydrogenase: linking endocrinology and metabolism in the endoplasmic reticulum. J Mol Endocrinol 2009;42:283–9. http://dx.doi.org/10.1677/JME-08-0156.
[14] Hewitt KN, Walker EA, Stewart PM. Minireview: hexose-6-phosphate dehydrogenase and redox control of 11{beta}-hydroxysteroid dehydrogenase type 1 activity. Endocrinology 2005;146:2539–43. http://dx.doi.org/10.1210/en.2005-0117.
[15] Marcolongo P, Piccirella S, Senesi S, Wunderlich L, Gerin I, Mandl J, et al. The glucose-6-phosphate transporter-hexose-6-phosphate dehydrogenase-11beta-hydroxysteroid dehydrogenase type 1 system of the adipose tissue. Endocrinology 2007;148:2487–95. http://dx.doi.org/10.1210/en.2006-1472.
[16] Dzyakanchuk AA, Balázs Z, Nashev LG, Amrein KE, Odermatt A. 11beta-Hydroxysteroid dehydrogenase 1 reductase activity is dependent on a high ratio of NADPH/NADP(+) and is stimulated by extracellular glucose. Mol Cell Endocrinol 2009;301:137–41. http://dx.doi.org/10.1016/j.mce.2008.08.009.
[17] Lavery GG, Walker EA, Draper N, Jeyasuria P, Marcos J, Shackleton CHL, et al. Hexose-6-phosphate dehydrogenase knock-out mice lack 11 beta-hydroxysteroid dehydrogenase type 1-mediated glucocorticoid generation. J Biol Chem 2006;281:6546–51. http://dx.doi.org/10.1074/jbc.M512635200.
[18] Park J, Rho HK, Kim KH, Choe SS, Lee YS, Kim JB. Overexpression of glucose-6-phosphate dehydrogenase is associated with lipid dysregulation and insulin resistance in obesity. Mol Cell Biol 2005;25:5146–57. http://dx.doi.org/10.1128/MCB.25.12.5146-5157.2005.
[19] Rask E, Walker BR, Söderberg S, Livingstone DEW, Eliasson M, Johnson O, et al. Tissue-specific changes in peripheral cortisol metabolism in obese women: increased adipose 11beta-hydroxysteroid dehydrogenase type 1 activity. J Clin Endocrinol Metab 2002;87:3330–6. http://dx.doi.org/10.1210/jcem.87.7.8661.
[20] Vegiopoulos A, Herzig S. Glucocorticoids, metabolism and metabolic diseases. Mol Cell Endocrinol 2007;275:43–61. http://dx.doi.org/10.1016/j.mce.2007.05.015.
[21] Walker BR. Extra-adrenal regeneration of glucocorticoids by 11beta-hydroxysteroid dehydrogenase type 1: physiological regulator and pharmacological target for energy partitioning. Proc Nutr Soc 2007;66:1–8. http://dx.doi.org/10.1017/S002966510700523X.
[22] Hecker PA, Lionetti V, Ribeiro RF, Rastogi S, Brown BH, O'Connell KA, et al. Glucose 6-phosphate dehydrogenase deficiency increases redox stress and moderately accelerates the development of heart failure. Circ Heart Fail 2013;6:118–26. http://dx.doi.org/10.1161/CIRCHEARTFAILURE.112.969576.
[23] Bashan N, Kovsan J, Kachko I, Ovadia H, Rudich A. Positive and negative regulation of insulin signaling by reactive oxygen and nitrogen species. Physiol Rev 2009;89:27–71. http://dx.doi.org/10.1152/physrev.00014.2008.
[24] Jankovic A, Korac A, Buzadzic B, Otasevic V, Stancic A, Daiber A, et al. Redox implications in adipose tissue (dys)function-A new look at old acquaintances. Redox Biol 2015;6:19–32. http://dx.doi.org/10.1016/j.redox.2015.06.018.
[25] London E, Castonguay TW. High fructose diets increase 11β-hydroxysteroid dehydrogenase type 1 in liver and visceral adipose in rats within 24-h exposure. Obesity (Silver Spring) 2011;19:925–32. http://dx.doi.org/10.1038/oby.2010.284.
[26] Alberts P, Rönquist-Nii Y, Larsson C, Klingström G, Engblom L, Edling N, et al. Effect of high-fat diet on KKAy and ob/ob mouse liver and adipose tissue corticosterone and 11-dehydrocorticosterone concentrations. Horm Metab Res 2005;37:402–7. http://dx.doi.org/10.1055/s-2005-870228.
[27] Gonzalo-Lumbreras R, Muñiz-Valencia R, Santos-Montes A, Izquierdo-Hornillos R. Liquid chromatographic method development for steroids determination (corticoids and anabolics). Application to animal feed samples. J Chromatogr A 2007;1156:321–30. http://dx.doi.org/10.1016/j.chroma.2007.01.095.
[28] Fraga CG, Leibovitz BE, Tappel AL. Halogenated compounds as inducers of lipid peroxidation in tissue slices. Free Radic Biol Med 1987;3:119–23.
[29] Lang JK, Packer L. Quantitative determination of vitamin E and oxidized and reduced coenzyme Q by high-performance liquid chromatography with in-line ultraviolet and electrochemical detection. J Chromatogr 1987;385:109–17.

[30] Rousseau I, Galleano M, Puntarulo S. Fe allocation in liver during early stages of endotoxemia in Fe-overload rats. Toxicol Pathol 2011;39:1075–83. http://dx.doi.org/10.1177/0192623311425057.
[31] Anderson ME. Determination of glutathione and glutathione disulfide in biological samples. Methods Enzymol 1985;113:548–55.
[32] Boveris A, Fraga CG, Varsavsky AI, Koch OR. Increased chemiluminescence and superoxide production in the liver of chronically ethanol-treated rats. Arch Biochem Biophys 1983;227:534–41.
[33] Aebi H. Catalase in vitro. Methods Enzymol 1984;105:121–6.
[34] Carlberg I, Mannervik B. Glutathione reductase. Methods Enzymol 1985;113:484–90.
[35] Flohé L, Günzler WA. Assays of glutathione peroxidase. Methods Enzymol 1984; 105:114–21.
[36] Li J-M, Wheatcroft S, Fan LM, Kearney MT, Shah AM. Opposing roles of p47phox in basal versus angiotensin II-stimulated alterations in vascular O2- production, vascular tone, and mitogen-activated protein kinase activation. Circulation 2004; 109:1307–13. http://dx.doi.org/10.1161/01.CIR.0000118463.23388.B9.
[37] Faulconnier Y, Thévenet M, Fléchet J, Chilliard Y. Lipoprotein lipase and metabolic activities in incubated bovine adipose tissue explants: effects of insulin, dexamethasone, and fetal bovine serum. J Anim Sci 1994;72:184–91.
[38] Simpson IA, Yver DR, Hissin PJ, Wardzala LJ, Karnieli E, Salans LB, et al. Insulin-stimulated translocation of glucose transporters in the isolated rat adipose cells: characterization of subcellular fractions. Biochim Biophys Acta 1983;763:393–407.
[39] Rogoff D, Black K, McMillan DR, White PC. Contribution of hexose-6-phosphate dehydrogenase to NADPH content and redox environment in the endoplasmic reticulum. Redox Rep 2010;15:64–70. http://dx.doi.org/10.1179/174329210X12650506623249.
[40] Zhang Z, Yu J, Stanton RC. A method for determination of pyridine nucleotides using a single extract. Anal Biochem 2000;285:163–7. http://dx.doi.org/10.1006/abio.2000.4701.
[41] Tian WN, Braunstein LD, Pang J, Stuhlmeier KM, Xi QC, Tian X, et al. Importance of glucose-6-phosphate dehydrogenase activity for cell growth. J Biol Chem 1998;273: 10609–17.
[42] Dornas WC, de Lima WG, Pedrosa ML, Silva ME. Health implications of high-fructose intake and current research. Adv Nutr 2015;6:729–37. http://dx.doi.org/10.3945/an.114.008144.
[43] Senesi S, Legeza B, Balázs Z, Csala M, Marcolongo P, Kereszturi E, et al. Contribution of fructose-6-phosphate to glucocorticoid activation in the endoplasmic reticulum: possible implication in the metabolic syndrome. Endocrinology 2010;151:4830–9. http://dx.doi.org/10.1210/en.2010-0614.
[44] Zubiría MG, Fariña JP, Moreno G, Gagliardino JJ, Spinedi E, Giovambattista A. Excess fructose intake-induced hypertrophic visceral adipose tissue results from unbalanced precursor cell adipogenic signals. FEBS J 2013;280:5864–74. http://dx.doi.org/10.1111/febs.12511.
[45] Taghibiglou C, Carpentier A, Van Iderstine SC, Chen B, Rudy D, Aiton A, et al. Mechanisms of hepatic very low density lipoprotein overproduction in insulin resistance. Evidence for enhanced lipoprotein assembly, reduced intracellular ApoB degradation, and increased microsomal triglyceride transfer protein in a fructose-fed hamster model. J Biol Chem 2000;275:8416–25.
[46] Havel PJ. Dietary fructose: implications for dysregulation of energy homeostasis and lipid/carbohydrate metabolism. Nutr Rev 2005;63:133–57.
[47] Janevski M, Ratnayake S, Siljanovski S, McGlynn MA, Cameron-Smith D, Lewandowski P. Fructose containing sugars modulate mRNA of lipogenic genes ACC and FAS and protein levels of transcription factors ChREBP and SREBP1c with no effect on body weight or liver fat. Food Funct 2012;3:141–9. http://dx.doi.org/10.1039/c1fo10111k.
[48] Tran LT, Yuen VG, McNeill JH. The fructose-fed rat: a review on the mechanisms of fructose-induced insulin resistance and hypertension. Mol Cell Biochem 2009; 332:145–59. http://dx.doi.org/10.1007/s11010-009-0184-4.
[49] Schröder K, Wandzioch K, Helmcke I, Brandes RP. Nox4 acts as a switch between differentiation and proliferation in preadipocytes. Arterioscler Thromb Vasc Biol 2009;29:239–45. http://dx.doi.org/10.1161/ATVBAHA.108.174219.
[50] Tormos KV, Anso E, Hamanaka RB, Eisenbart J, Joseph J, Kalyanaraman B, et al. Mitochondrial complex III ROS regulate adipocyte differentiation. Cell Metab 2011;14:537–44. http://dx.doi.org/10.1016/j.cmet.2011.08.007.
[51] Park J, Choe SS, Choi AH, Kim KH, Yoon MJ, Suganami T, et al. Increase in glucose-6-phosphate dehydrogenase in adipocytes stimulates oxidative stress and inflammatory signals. Diabetes 2006;55:2939–49. http://dx.doi.org/10.2337/db05-1570.
[52] Bujalska IJ, Walker EA, Hewison M, Stewart PM. A switch in dehydrogenase to reductase activity of 11 beta-hydroxysteroid dehydrogenase type 1 upon differentiation of human omental adipose stromal cells. J Clin Endocrinol Metab 2002;87: 1205–10. http://dx.doi.org/10.1210/jcem.87.3.8301.
[53] Atanasov AG, Nashev LG, Schweizer RAS, Frick C, Odermatt A. Hexose-6-phosphate dehydrogenase determines the reaction direction of 11beta-hydroxysteroid dehydrogenase type 1 as an oxoreductase. FEBS Lett 2004;571:129–33. http://dx.doi.org/10.1016/j.febslet.2004.06.065.
[54] Legeza B, Balázs Z, Odermatt A. Fructose promotes the differentiation of 3T3-L1 adipocytes and accelerates lipid metabolism. FEBS Lett 2014;588:490–6. http://dx.doi.org/10.1016/j.febslet.2013.12.014.
[55] Bursać BN, Djordjevic AD, Vasiljević AD, Milutinović DDV, Veličković NA, Nestorović NM, et al. Fructose consumption enhances glucocorticoid action in rat visceral adipose tissue. J Nutr Biochem 2013;24:1166–72. http://dx.doi.org/10.1016/j.jnutbio.2012.09.002.
[56] Kovačević S, Nestorov J, Matić G, Elaković I. Dietary fructose-related adiposity and glucocorticoid receptor function in visceral adipose tissue of female rats. Eur J Nutr 2014;53:1409–20. http://dx.doi.org/10.1007/s00394-013-0644-1.
[57] Veličković N, Djordjevic A, Vasiljević A, Bursać B, Milutinović DV, Matić G. Tissue-specific regulation of inflammation by macrophage migration inhibitory factor and glucocorticoids in fructose-fed Wistar rats. Br J Nutr 2013;110:456–65. http://dx.doi.org/10.1017/S0007114512005193.